RAFFLES BULLETIN OF ZOOLOGY **70**: 289–304
Date of publication: 6 May 2022
DOI: 10.26107/RBZ-2022-0013
http://zoobank.org/urn:lsid:zoobank.org:pub:C227D6E3-A0B5-41DC-B7E3-23C0E9A91057

Javan mongoose (*Herpestes javanicus*) abundance and spatial ecology in a degraded dry dipterocarp forest

Sarah **Sherburne**[1*], Wyatt Joseph **Petersen**[1], Marnoch **Yindee**[2], Tommaso **Savini**[1] & Dusit **Ngoprasert**[1]

Abstract. Southeast Asia is rich in small carnivore species, but baseline information on these species is frequently lacking. Many of the region's remaining forests are degraded, which can drastically change ecosystem function and structure. The Javan mongoose is a small generalist carnivore with a wide distribution across Southeast Asia, whose population, home-range size, and micro-habitat selection are poorly known. We investigated each within a degraded forest fragment in Northeast Thailand using a multimethod approach involving camera trap and radio telemetry data. We found mongoose abundance was positively associated with dry dipterocarp forest (DDF) and has a negative relationship with basal area of small trees (diameter at breast height < 10 cm). Across our entire study site, we found a mean abundance of 1.10 animals per sampling station (SE 0.30 95% CI 0.65–1.92) and within the DDF we found 3.04 animals per station (SE 0.75 95% CI 1.87–4.96). The mean home-range size for two males was 1.86 km^2 and for one female was 0.27 km^2. Availability of termite mounds with entry holes was our top model for den site selection. Prey availability did not affect micro-habitat selection by mongoose, presumably due to an even distribution of small mammals across the DDF. Mongoose selected for areas with low numbers of small trees, indicating an avoidance of closed forest environments. Our findings indicate that Javan mongoose select for open dry forest and can tolerate moderate forest degradation.

Key words. home-range estimate, Auto-correlated Kernel Density Estimation, habitat selection, den site selection, radio telemetry

INTRODUCTION

Southeast Asia has a disproportionately high level of small carnivore (< 16 kg) species when compared to other regions, according to the International Union for Conservation of Species (IUCN) (Marneweck et al., 2021). Habitat changes such as deforestation for agricultural use impacts small carnivores species worldwide, and Southeast Asia has among the fastest worldwide deforestation rates, with only 35% of old-growth forest left as of 2015 and many remaining forests being both degraded and fragmented (Sodhi et al., 2010; Wilcove et al., 2013; Taubert et al., 2018; Estoque et al., 2019; Grantham et al., 2020). Deforestation degrades habitat by altering forest structure and ecosystem functions and can affect habitat choice and use by its inhabiting species, as the ability of species to choose 'ideal' habitats is diminished (Delciellos et al., 2017; Vanbianchi et al., 2017). Small carnivores show a variable response to degradation; most species are negatively affected (Mudappa et al., 2007; Marneweck et al., 2021) while some show the ability to adapt to it (Deuel et al., 2017; Ramesh et al., 2017). Unfortunately, basic ecological data are not available for many small carnivore species (Brooke et al., 2014), therefore their response to habitat degradation is not easily predicted.

The Javan mongoose (*Herpestes javanicus*) is found throughout Southeast Asia, with recorded distributions ranging from Indonesia to the western edge of China (Chutipong et al., 2016). The IUCN considers the Javan mongoose to be of Least Concern because of its perceived abundance, apparent widespread distribution, and the fact that there are recorded occurrences in degraded habitats and agricultural areas (Duckworth et al., 2010; Chutipong et al., 2016). However, data on the species' actual distribution are limited to anecdotal sightings and non-targeted camera trap surveys mainly within protected areas (Chutipong et al., 2014). As a result, no detailed status assessments have been undertaken to date and little is known about the species' distribution, ecology, or abundance throughout its wide range. This lack of assessment is partly due to a recent taxonomic separation from the extensively introduced small Indian mongoose (*Herpestes auropunctatus*), which has been widely studied in island environments due to its deleterious ecological effects on native species within its introduced range (Lowe et al., 2004; Veron & Jennings, 2017). However, the findings from these island studies are not necessarily transferable to native populations, as the

Accepted by: Norman Lim T-Lon

[1]Conservation Ecology Program, King Mongkut's University of Technology Thonburi, 49 Thakham, Bangkhuntien, Bangkok, 10150 Thailand; Email: sr.sherburne@gmail.com (*corresponding author)

[2]Akkhraratchakumari Veterinary College, Walailak University 222 Thaiburi, Thasala District, Nakhon Si Thammarat 80160, Thailand

ISSN 2345-7600 (electronic) | ISSN 0217-2445 (print)

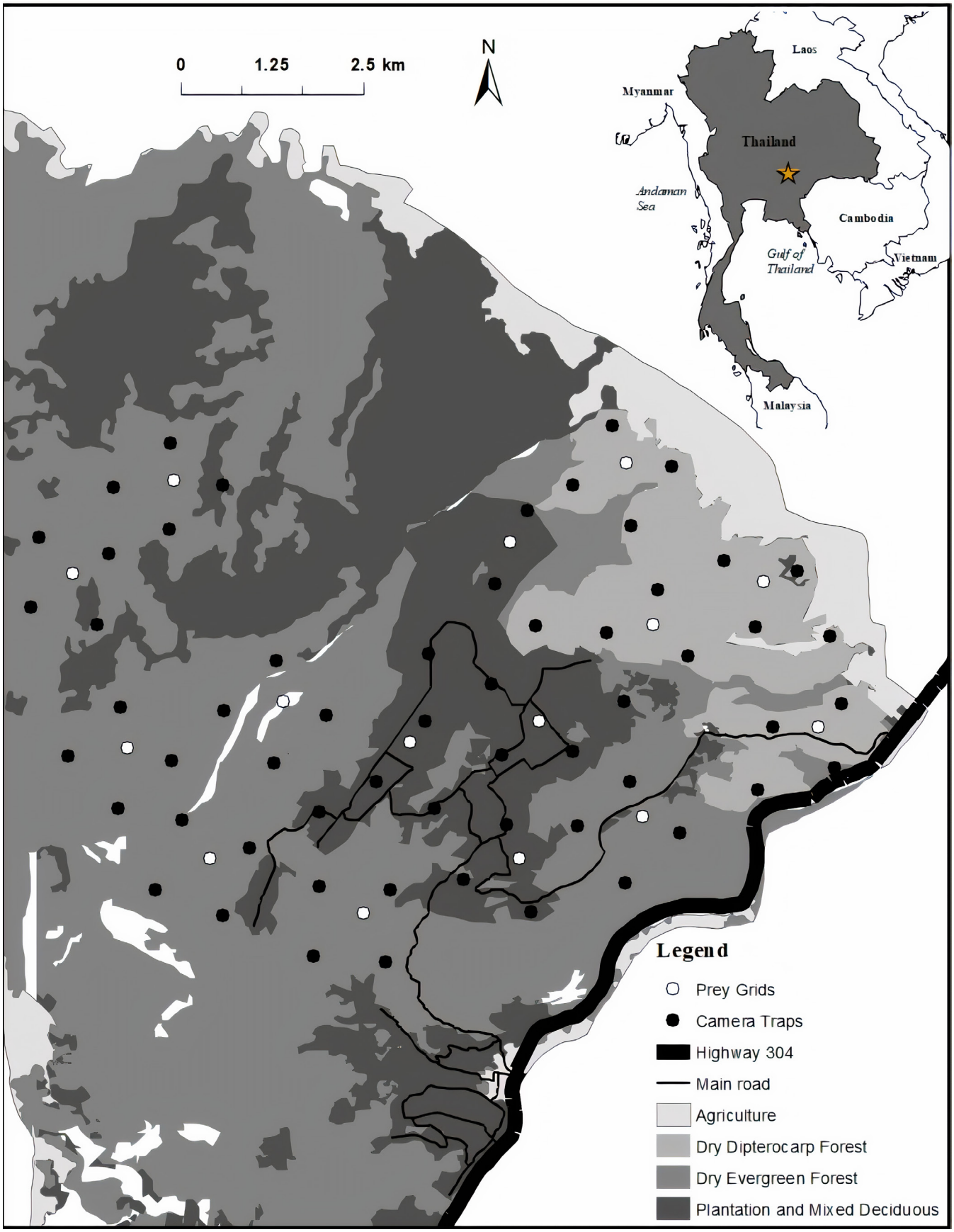

Fig. 1. Map and location of Sakaerat Biosphere Reserve with camera trap stations used to estimate Javan mongoose (*Herpestes javanicus*) abundance in 2017. Prey grid stations were used to calculate yearly averaged rodent biomass from January 2017 to November 2017.

ecological conditions in island environments are often very different from native environments. For example, density estimates for small Indian mongoose average 51–64 times higher in introduced ranges, and reproductive features are significantly different (Owen & Lahti, 2020).

Studies on the Javan mongoose, and indeed on most Asian mongooses, are sparse in their native range, and more information is needed to understand if this species is threatened by habitat degradation. This study aims to investigate Javan mongoose ecology in a forest fragment to inform conservation planning. We considered three different aspects of its ecology: a) abundance, b) home-range size, and c) micro-habitat selection. Abundance was chosen because low abundance is correlated with high risk of extinction (Mace et al., 2008) and it allows for comparisons between habitats. Home-range size and micro-habitat selection was investigated because they can inform habitat requirements within human modified landscapes (Hinton et al., 2016; Filla et al., 2017). We investigated home-range size via radio telemetry and predicted that it would be larger in males than females, as Javan mongoose show sexual dimorphism, which can indicate polygamy in mammals and greater 'ranging' for mating access (Simberloff et al., 2000; McPherson & Chenoweth, 2012). To inform our micro-habitat selection we recorded vegetation characteristics, prey availability, and den abundance in selected and available habitats. We collected prey abundance data as it can be a strong predictor for mesocarnivores and is most accurate when measured directly as opposed to using habitat with suitable characteristics for high prey density as a surrogate (Wolff et al., 2015). Selection for high prey abundance must be weighed against exposure to predation and competition for high resource areas, so whether individuals select for or against it can be informative (Case & Bolger, 1991; Suraci et al., 2016). Den sites and their relative availability can also factor in micro-habitat selection by small carnivores, since den availability can decrease predation and improve reproductive success through safe rearing of young (Tannerfeldt et al., 2003; Moehrenschlager et al., 2007). We predicted that on the micro-habitat level, mongoose would select areas with a higher relative biomass of prey resources and a larger number of potential den sites to decrease predation risk and increase reproductive success.

METHODS

Study Site. The study was conducted at Sakaerat Biosphere Reserve (14.44–14.55°N, 101.88–101.95°E) in northeastern Thailand. Elevation ranges 250–762 metres above sea level. Total forested area is 148 km^2, with dry dipterocarp forest (DDF) comprising 11%, and the other two major forest types being dry evergreen forests (54%) and plantation (33%) (Petersen et al., 2019). The DDF is bordered by agricultural areas to the east and closed canopy dry evergreen forest and reforested areas to the west. It is split in the southern portion by a segment of dry evergreen forest (Fig. 1). Our site has a tropical climate characterised by a wet and dry season. We defined the wet season as May to October (average rainfall of 920 mm) and the dry season as November to April (average rainfall of 220 mm) for the reserve (Khamcha et al., 2018). DDF is burned yearly during the dry season by the reserve's staff. The reserve is now a protected zone, but prior to 1977, much of the original forest had been converted to plantations and fields and undergone severe deforestation, and the remaining forest is still recovering (Ongsomwang & Sutthivanich, 2014). The reserve is bordered on the southern side by a major highway, on the northern side by a reservoir, and on the eastern and western sides by agricultural areas.

Camera trapping. Sixty camera traps (SG565, Scout Guard) were deployed across Sakaerat Biosphere Reserve to sample small carnivore species from January 2017 to October 2017 covering 65 km^2 of major forest types. Traps were deployed in a stratified random manner by forest type, with a minimum distance of 1 km between camera-trap stations (dry evergreen forest: 28 traps covering 34 km^2; dry dipterocarp forest: 16 traps covering 16 km^2; reforested areas: 16 traps covering 15 km^2, Fig. 1). Cameras were secured to the closest available tree to the site coordinates, 3 metres from the target zone and 45 cm above the ground. Cameras were left active 24 hours a day. Fish oil scent lures were placed in 325 ml aluminum cans buried flush to the ground in the focal area of each camera. Scent lures were used because they have been shown to increase the probability of detection for mesopredators without affecting abundance estimates (Gerber et al., 2012; Ferreras et al., 2018; Holinda et al., 2020). Cameras were revisited once per month for battery, SD card, and lure replacement. Mongoose detections were considered notionally independent when the time between photographs was ≥ 30 minutes (O'Brien et al., 2003). We constructed a binary detection history (i.e., detect/not-detect) using daily occasions (0000–2359 h). Trap nights were defined as the number of daily occasions where cameras were functioning.

Mongoose abundance estimations. We estimated mongoose abundance using the Royle-Nichols model (RN model), which utilises repeated observations of unmarked animals in detected/non-detected data (Royle & Nichols, 2003; Kalle et al., 2014; Paolino et al., 2018). The model has two parameters to be estimated: 1) mean abundance per sampling station (λ), which can be interpreted as the number of mongoose home ranges overlapping one of our camera traps, and 2) the probability of detecting a species at a sampling station (p) (Royle & Nichols, 2003; Nakashima, 2020). The RN model calculates abundance as an analogue to uneven detection probability, while incorporating the effects of both site-specific covariates and observed (sampling) covariates. All analysis was done in program R 4.0.5 (R Core Team, 2020). Abundance estimates were made using the 'unmarked' package (Fiske & Chandler, 2011). The number of days after each scent lure refuelling was used as a sampling covariate to account for differences in detection probability across sampling days. We subset our camera trap data to the first 180 occasions to meet the closure assumption. To model differences in forest structure that could affect abundance, we collected small tree basal area, large tree basal area, and canopy cover percentage (Table 1). These three abundance covariates were collected at ten-metre plots centred on each

Table 1. Descriptions of covariates used in micro-habitat selection models, den site selection models, and abundance estimation models. Habitat variables were collected from 15-metre radius plot for micro-habitat selection variables and 10-metre radius plots for abundance variables. Plots were centred on radio tracked mongoose locations or camera trap stations, respectively. Prey variables were collected from prey grids and averaged (Figs. 1, 2).

Micro-habitat and den site selection variables		
Variables	**Name**	**Description and Measurement Unit**
Mean basal area of small trees	avgBasalSmall	Mean basal area for small trees (DBH ≤ 10 cm) (cm^2)
Mean basal area of large trees	avgBasalLarge	Mean basal area for large trees (DBH > 10 cm) (cm^2)
Shrub Count	shrubCount	Number of shrubs < 3 cm DBH and ≥ 50 cm height
Termite Mound with Entry	termiteAvailable	Number of termite mounds with entry holes
Termite Mound without Entry	termiteNonavailable	Number of termite mounds without entry holes
Holes	holes	Number of dug holes ≥ 4 cm diameter
Small tree count	smallTreeCount	Number of trees (DBH ≤ 10 cm)
Large tree count	largeTreeCount	Number of trees (DBH > 10 cm)
Total tree count	totalTrees	Sum of all trees in plot
Average Rodent Biomass	avgRodentBiomass	Average mass of large rodent species for grid multiplied by large rodent species density for grid + average mass of small rodent species for grid multiplied by small rodent species density for grid. Averaged per habitat zone. (g/ha)
Pitfall invertebrate mass	insectPitfall	Sum of dry mass for invertebrates collected by pitfall trap per habitat zone (g)
Total prey	totalPrey	Sum of pitfall invertebrate mass, average rodent biomass and sweep invertebrate mass (g)
Sweep net invertebrate mass	insectSweep	Sum of dry mass for invertebrates collected by sweep netting per habitat zone (g)
FAI	FAI	Average basal large multiplied by large tree count (cm^2)
Abundance estimation variables		
Average rodent biomass	rAvg	Averaged bimonthly rodent biomass (g/ha) value over wet and dry season
small trees basal area	basalS	Average basal area for all small trees (DBH < 10 cm) within each camera-trap station's two micro-habitat plots, multiplied by the density of trees (DBH < 10 cm) within the same plots. Scaled to m^2/ha.
large trees basal area	basalL	Average basal area for all large trees (DBH ≥ 10 cm) within each camera-trap station's two micro-habitat plots, multiplied by the density of trees (DBH ≥ 10 cm) within the same plots. Scaled to m^2/ha.
Canopy cover	cc	Percent canopy cover
Road	road	Distance to nearest road (m)
Edge	edge	Distance to edge of Sakaerat Biosphere Reserve (m)
Oil	oil	Date from deployment of fish oil scent lure to replacement

camera trap station. To model how disturbance might affect abundance, we calculated the distance to roads and the edge of Sakaerat Biosphere Reserve's boundary for each point.

Covariates were tested for pairwise correlation using the 'corplot' package (Wei & Simko, 2021). Covariates with correlation values greater than 0.5 were not included within the same model. Continuous data were standardised using the 'scale' function (mean = 0, sd = 1) in R. We tested the default upper summation index for latent abundance (K = 25) to ensure that it will not affect parameter estimates by comparing approximate small sample size corrected Akaike Information Criterion (AICc) values between K=25, K=50 and K=100. We found that the default value of 25 was sufficient for our data.

Best fitting models for abundance were selected using AICc (Burnham et al., 2011). To test the goodness of fit for our RN models, we followed the MacKenzie & Bailey (2004) methodology of parametric bootstrapping using three tests: sum-of-squared errors, chi-square, and Freeman–Tukey (Paolino et al., 2018). We generated 1,000 bootstrapped resamples and tested the fit of the most parameterised (global) model with our detection covariate (fish oil) and our

Fig. 2. Forest types in Sakaerat Biosphere Reserve: A, dry dipterocarp forest; B, dry evergreen forest

abundance covariates (basalS+rAvg+basalB+edge+road) in the models. We also calculated an overdispersion ratio (ĉ) for our global model to test for possible overdispersion in our detection history (Burnham & Anderson, 1998). In order to ensure our detections were independent among samples, we tested for spatial autocorrelation in our data using the Moran's I test in the 'ape' package (Paradis & Schliep, 2019). We created an inverted distance matrix of our camera trap locations and used relative abundance index (number of independent photographs per station) as our value. With a *P*-value of > 0.05, the hypothesis that there is significant spatial correlation is not supported. We estimated mean abundance for our trapping area by predicting λ_i for each of our camera trap stations based on estimates from our top model using the 'predict' function in R. We then calculated the mean of overall stations.

Trapping and radio tracking. Mongoose trapping was carried out from December 2019 to January 2021. A total of 11 large live traps (121 × 50 cm) and 34 (24 × 9.5; 31 × 10 cm) small live traps were used to capture mongooses, for a total of 110 trap sites. Traps were left in place for a minimum of 7 days unless disturbed by dogs, in which case traps were moved immediately. Trapping sites were within the DDF and placed according to our camera trap data for high mongoose detection within Sakaerat. In addition, we selected sites based on recent mongoose sightings, the presence of tracks, and high quantity of potential den sites such as termite mounds. Live traps were baited with a chicken carcass and left open for 24 hours and checked every morning.

For each individual captured, we recorded body length, body condition, sex, and age class (Appendix 1) before collaring them with VHF collars model M1-2A from Holohil Systems limited, with built-in activity sensors. Mongooses were immobilised using Zoletil general anaesthetic to allow for measurements and collar fitting while minimising stress (Zoletil the Versatile Anaesthetic, 2021) (see Appendix 2). A leather harness system was added to help with collar retention. All VHF collars (31 g) with harnesses were approximately five percent or less of the animal's mass (Sikes & Gannon, 2011). Age class was determined by the condition of the teeth (worn teeth indicating old age), descended testes for males, and condition of the nipples in females. Post-processing, individuals were kept within the live trap until fully recovered from sedation, and then released at their capture location.

Collared mongooses were located up to two times a day. Radio tracking was done on foot using a two-element antenna and an ATS receiver model R410. Due to tall grasses in the DDF (Fig. 2), visual sightings of collared mongoose were rare. Locations for individuals were determined using triangulation, with three lines of intersection from a distance of 20 metres or less. We allowed a minimum of three hours to pass between tracks to decrease temporal autocorrelation between points. For each location we recorded habitat type, observer distance, and whether the collar's activity sensor was activated.

If a collar's activity sensor did not indicate movement during the tracking, we approached to see if the mongoose was sheltering in a den site. We waited for inactivity to ensure actual selection of a den, and to minimise disruption if the mongoose was foraging. The type of den, number of entrances, entrance dimensions, and number of days the den was visited were all recorded.

Home-range estimation. Home-range estimations were calculated using Auto-correlated Kernel Density Estimation (AKDE) to incorporate potential temporal or positional autocorrelation (Fleming et al., 2015; Noonan et al., 2019). AKDE analysis was done using the R package 'ctmm' (Calabrese et al., 2016). We used a variogram to plot a semi-variance function, which visualised autocorrelation in our data by plotting the average square displacement unit (hectares) over a time lag period (months). We then applied a variety of continuous-time stochastic movement models to each individual's telemetry data. Models tested include Ornstein–Uhlenbeck motion (Brownian motion within a home-range), Ornstein–Uhlenbeck with foraging, and independent identical distribution (no autocorrelation) (Fleming et al., 2014). We compared AICc values to determine the best fitting movement

mode model for each individual (Burnham et al., 2011). All home-ranges were calculated at 95% utilisation distribution and its 95% confidence interval. We also calculated a 50% utilisation distribution as a proxy for an individual's 'core area'. All analysis was completed in program R 4.0.5 (R Core Team, 2020).

Micro-habitat selection. We collected vegetation variables in areas used by mongooses and compared them to available locations to determine the micro-habitat selection of radio-collared mongooses. Used locations were chosen by randomly selecting radio telemetry locations. We collected micro-habitat data on 50 used and 100 available locations for each of our male mongooses, and 40 used and 80 available for the female. For available locations, we collected a plot 100 metres to the north and south of each used location. Aside from characteristics of den sites, identical variables were collected for both general micro-habitat plots and den site plots.

At each location we established a 15-m radius circular plot. We collected ground cover percentage, diameter at breast height (DBH) for trees ≥ 3 cm DBH, count of shrubs and saplings < 3 cm in diameter and ≥ 50 cm in height, and potential den site type and count (Table 1). Shrubs less than 50 cm height were at the same height as the primary groundcover (*Arundinaria pusilla*) and were considered functionally groundcover and not included in shrub count. Trees were subset in the analysis as 'small' or 'large', large being > 10 cm DBH and small between 3–10 cm DBH. Ground cover, understorey (shrub and sapling) count, and den site availability were recorded as an indication of potential cover and refuge site availability. Number of trees and DBH were recorded to indicate undisturbed forested area versus open or edge habitat, as tree size varies within each. To compare habitat features across the DDF, we labelled micro-habitat plots as plots near the edge (< 400 metres from edge) or core DDF (≥ 400 metres from edge).

We ran logistic regression models using the 'lme4' package (Bates et al., 2015) in R to determine mongoose selection based on micro-habitat features and prey availability. Prior to data analysis, we tested for outliers, correlation among variables, and standardised the continuous variables (see above). We tested the inclusion of mongoose ID as a random effect on our variables and found no change in the outcome, while decreasing the parsimony of the model and therefore we chose not to include mongoose ID as a random effect. Top models were selected using AICc values. We validated our top models by calculating the area under the receiver operator characteristic curve (AUC) for model averaged predictions in the R package 'PresenceAbsence' (Freeman & Moisen, 2008). Model averaging was done using the 'AICcmodavg' package (Mazerolle, 2020).

Prey biomass. A recent study by Subrata et al. (2021) provided evidence that rodents and arthropods occur frequently (83% and 100% frequency of occurrence, respectively) in the Javan mongoose's diet. We used biomass of these groups as a proxy for prey availability of mongoose, and averaged prey biomass was used as a covariate in our micro-habitat selection analysis.

Rodent prey biomass for abundance estimation was sampled during four periods in 2017 (February–March, April–May, July–August, September–October) at 15 sites (60 sessions in total; 7 sites in dry evergreen; 4 in dry dipterocarp; 4 in reforested). We used Sherman live traps (7.62 × 8.89 × 22.86 cm) placed on the ground. At each of the 15 sites, we arranged 25 live traps in a 5 × 5 grid with 20 m spacing between traps. Sites were sampled once every two months, with each bimonthly session lasting seven consecutive trap nights. Traps were baited with peanut butter and checked once a day in the morning. Captured animals were uniquely marked with an ear tag, weighed, and then released at their capture site. The mean mass of rodents captured each session was multiplied by the session's density estimate to obtain session biomass. Yearly averaged biomass estimates from each small mammal trapping session were assigned as a covariate to the nearest 4 camera-trap stations within the same habitat type. For further details, see Petersen et al. (2019).

Prey biomass for micro-habitat selection was collected between October–December 2020. Prey grids were selected to represent habitat used by radio tracked mongoose, which was within the DDF. Our study area contains only a small fragmented portion of DDF surrounded by dry evergreen forest and agricultural areas (Fig. 1). We determined that edge type is therefore likely to affect prey distribution. We placed our prey grids in three different sections within the DDF, representing DDF adjacent to dry evergreen edge (DDF-dry evergreen edge), core DDF habitat, and DDF adjacent to agricultural areas (DDF-agricultural edge) (Fig. 3). All prey grids were sampled for eight consecutive days using 25 live traps in a 5 × 5 grid with 20 m spacing between traps. Prey grids were spaced ≥ 500 metres from one another. Edge grids were placed < 200 metres from their respective edge type to ensure that edge effect was represented. Core DDF zone grids were ≥ 400 metres from any other habitat.

For rodent capture, Sherman live traps (9.5 cm × 24 cm; 31 cm × 10 cm) were baited with peanut butter and checked once per day (12 rodent sites total; 3 in DDF-agricultural edge; 4 in the core DDF; 5 in the DDF-dry evergreen edge). Rodents were sampled using mark-recapture methods. For the first capture, each rodent was identified to the species-level, sexed, weighed, and uniquely marked with an identifying ear tag before release. All traps were placed on the ground and shaded with vegetation.

Rodent density (individuals/hectare) was calculated using the 'secr' package in R programming (Efford, 2021). Spatially explicit capture recaptures (SECR) allows for the calculation of density while accommodating heterogeneous probability of capture for individuals (Borchers, 2012). We plotted first captured mass of each individual by species and separated them into large (> 50 g average) and small (< 50 g average) groups. These groups were analysed separately to accommodate potentially different behavioural responses and home range sizes. Species groups were modelled in a

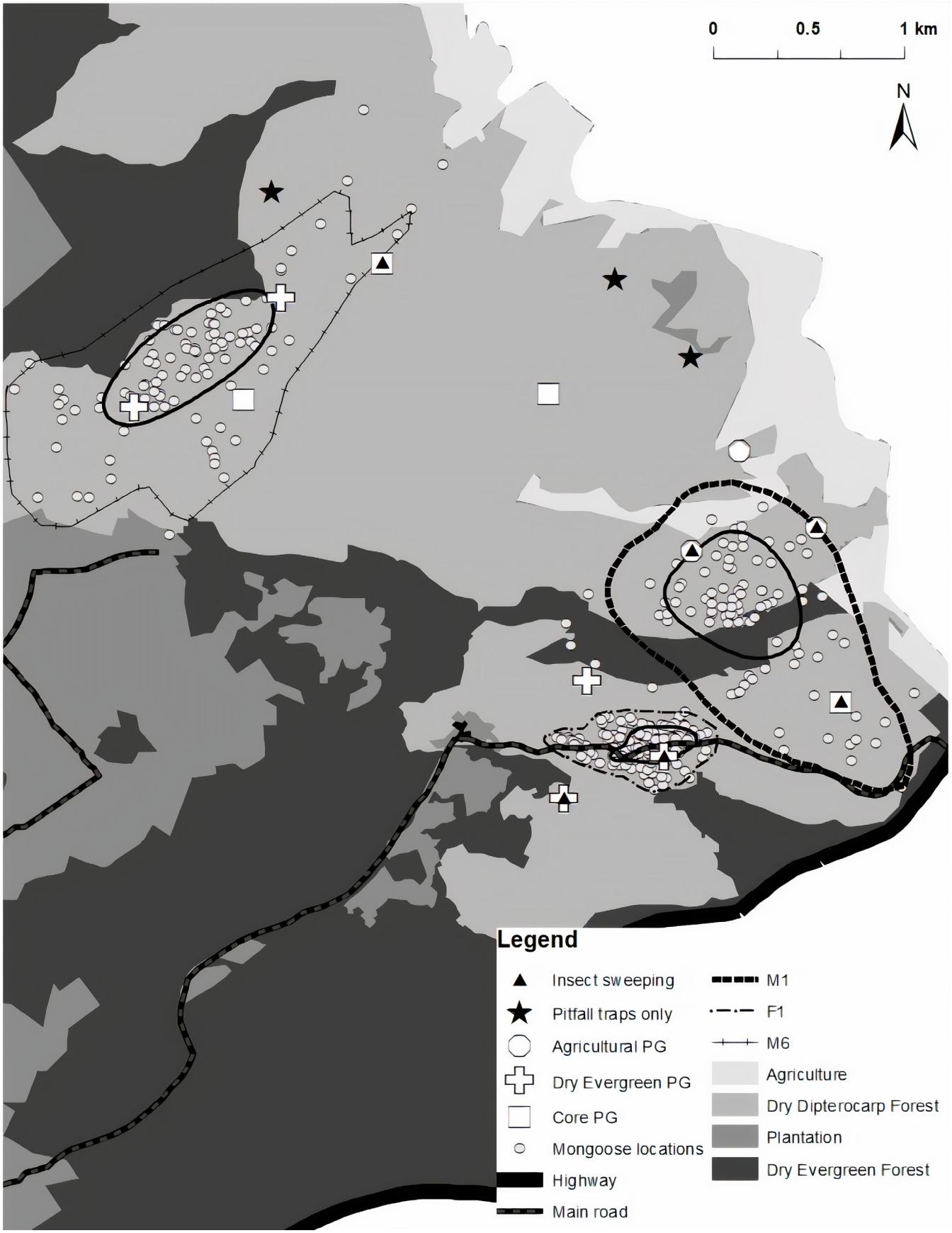

Fig. 3. Map of Sakaerat Biosphere Reserve with radio tracked (December 2019 to January 2021) Javan mongoose (*Herpestes javanicus*) home ranges and prey grids (PG). 95% utilisation contours (U.C) for male (M6, M1) and female (F1) mongooses are labelled in the legend. 50% U.C are solid line circles within each individual's home range. Prey grids collected ground-dwelling invertebrate mass as well as rodent biomass within the DDF (October to December 2020). Stars indicate where only ground-dwelling invertebrates were collected. Triangles indicate areas where sweep netting for invertebrates occurred in addition to sampling for rodent biomass and ground-dwelling invertebrates.

multi-session analysis, with each grid representing a separate session. For each session and group, we calculated sigma (σ, a parameter of movement derived from distance between individual's recapture locations) and g_0 (the probability of capture at an individual's activity centre), to derive estimated density.

To accommodate behavioural responses to trapping that may affect g_0, we incorporated potential lingering or transient 'trap shy' and 'trap happy' responses into our models. Models tested included: 1) a global lingering change in behaviour after first capture (*b*); 2) a global change in behaviour depending on capture during the previous occasion (*B*); 3) a trap-specific lingering response post initial capture (*bk*); 4) a transient trap-specific behaviour response post capture (*Bk*) (Efford, 2021). AICc scores were compared for all models to select the top-ranked model (Appendix 3). Density per grid for small and large species groups were estimated separately, multiplied by average mass for each group, and summed to calculate biomass per grid. Rodent biomass was used as a micro-habitat variable in selection analysis by calculating the average mass per habitat zone and assigning that zone's mass to micro-habitat plots within it.

Invertebrate biomass was collected using pitfall traps and sweep netting (15 pitfall sites: 5 in DDF-agricultural edge; 4 in core DDF; 6 in DDF-dry evergreen edge; 6 sweep net sites: 2 in each zone) (Fig. 3). With the exception of three grids, invertebrates and rodent biomass were collected at the same location. All pitfall grids followed the same layout as rodent trapping girds, 80-metre length transects in a five by five trap gird, with traps spaced 20 metres apart. A total of 25 pitfall traps per grid were placed. Sweep net collection took place walking alongside pitfall grids and was conducted within the same transects, with collection not exceeding the grid's layout. The collection took place upon arrival to the prey grid. For every 10 m along the sweep netting transect, 10 uninterrupted sweeps with a net were completed to collect flying insects. For pitfall traps, 15.7 cm deep plastic cups were dug flush to the ground, with two cups nesting within each other for easy removal. All invertebrates captured by either method were euthanised by being placed in a freezer overnight, and all large invertebrates were then stored in a 90% ethanol solution. Sweep net insects were stored in a freezer until drying. Dry weight of invertebrates was obtained by oven drying at 57°C for 24 hours. Gastropods were then deshelled and dried for an additional 5.5 hours till completely dry. Summed dry biomass (g) per habitat zone was calculated.

Den site selection. Den sites used by tracked mongoose were recorded and analysed separately from general micro-habitat plots. For variables collected and methods used to analyse den site selection, refer to the micro-habitat selection section (see above, and Table 1). For each den site used by mongoose, we collected den type, number of entry holes, and diameter of entry holes. Potential den sites were categorised as dug holes or termite mounds. Termite mounds with entry points and those without were categorised separately as 'non-available' (no entry holes) and 'available' (with entry holes). This allowed us to differentiate whether mongooses were simply selecting for termite rich areas or specifically for available den sites. Holes in termite mounds were assessed visually and deemed as viable entry points if they were the width of our smallest captured mongoose head or greater (diameter ≥ 4 cm).

RESULTS

Mongoose abundance. In the 8,867 trap nights considered for this study, we obtained 354 independent detections of Javan mongoose, 348 of which were within the DDF. For a full list of all mammals captured over the course of the study, see Petersen et al. (2019: appendix A). Our averaged rodent biomass was highest in dry evergreen forest and lowest in reforested area (dry evergreen = 458.3 g/ha, SE = 13.7; DDF = 287.5 g/ha, SE = 56.5; reforested area = 178.8 g/ha, SE = 22.6). We tested the addition of 'oil' as a covariate affecting detection probability and found that it decreased parsimony without adding to the model and so we chose not to include it (Table 2). For our parametric bootstrapped goodness of fit tests, the three generated *P*-values were all > 0.05. For our overdispersion ratio, our value was 0.55, suggesting the model adequately fit with the Poisson assumption. We ran our Moran's I test on data collected from traps within the DDF where our detections were grouped. We found that our data did not show significant spatial autocorrelation ($p > 0.05$).

Our best ranked model for mean abundance per sampling station (λ) was incorporating additive effects of basal area for both large and small trees and distance to Sakaerat Bioreserve edge (Table 2). Our λ_{mean} value for this model was 1.10 (SE 0.30, 95% CI 0.65–1.92). The greatest negative influence on abundance within this model was average basal area for trees with a diameter < 10 cm (β = -0.79, SE 0.28, 95% CI -1.34 to -0.24), followed by distance to edge (β = -0.70, SE 0.21, 95% CI -1.12 to -0.28) and then average basal area for trees with a diameter ≥ 10 cm (β = -0.52, SE 0.26, 95% CI -1.03 to -0.02). The probability of detection for our top model was 0.038 (SE 0.131, 95% CI 0.030–0.048). Because most (98%) of our observations were in DDF habitat, we calculated DDF specific λ_{mean} using our top model. Our DDF specific λ_{mean} was 3.04 (SE 0.75, 95% CI 1.87–4.96) and the range was 0.78–7.23.

Home-range estimation. We trapped a total of seven Javan mongoose over the course of the study, six males and one female (Appendix 1). Four males removed their radio collars within one to two days of release. A backpack system was added to help retain collars. Spatial data were collected for two adult males, M1 and M6, and one young adult female, F1, over the course of our tracking period (2 January 2019 to 14 September 2020). We collected 97 locations for M1, 194 locations for F1, and 101 locations for M6. M1 was not tracked from 9 February 2020 to 2 July 2020 due to a collar malfunction which led to data loss until recapture and collar replacement. Both M1 and F1 were predated by reticulated pythons (*Malayopython reticulatus*) during the tracking session (M1, 7 September 2020; F1, 31 March

Table 2. Model selection for Javan mongoose (*Herpestes javanicus*) abundance (λ) estimation and probability of detection (*p*) at Sakaerat Biosphere Reserve from January to June 2017, based on Royle-Nichols model. Definitions for covariates can be found in Table 1.

Models	***K***	**AICc**	**ΔAICc**	w_i
λ~basalL + basalS, p~1	5	2061.145	0.000	0.985
λ~basalL + basalS, p~1	4	2070.304	9.158	0.010
λ~basalS, p~1	3	2072.099	10.954	0.004
λ~cc+basalL, p~1	4	2078.338	17.193	0.000
λ~cc, p~1	3	2078.912	17.767	0.000
λ~edge, p~1	3	2080.395	19.250	0.000
λ~rAvg+cc, p~1	4	2080.465	19.319	0.000
λ~edge + road, p~1	4	2080.624	19.479	0.000
λ~cc+road, p~1	4	2080.757	19.612	0.000
λ~basalL, p~1	3	2110.377	49.232	0.000
λ~road, p~1	3	2112.222	51.077	0.000
λ~rAvg, p~1	3	2119.94	58.795	0.000
λ~constant, p~1	2	2122.554	61.409	0.000

K is the number of parameters included in the model, AICc is Akaike's Information Criteria corrected for small sample size, ΔAICc is the difference in AICc values, and w_i is the Akaike weight.

2020). M6's radio telemetry collar fell off at the end of the tracking period and was recovered.

For our two male mongooses, the most suitable movement mode for our data was independent identically distributed points, indicating little autocorrelation. For the female, Ornstein–Uhlenbeck anisotropic (random motion within a home-range) movement modes were deemed the best fit. Based on these movement modes, we chose a traditional kernel density estimator for our two males and an AKDE for the female in order to compensate for any autocorrelation. M1 had an estimated home-range area of 1.77 km^2 with a 95% CI of 1.24–2.38 km^2, and a core area of 0.34 km^2. M6 had an estimated home-range of 1.95 km^2 with a CI of 1.59–2.35 km^2, and a core area of 0.34 km^2. F1 had an estimated home-range area of 0.27 km^2 with CI of 0.22–0.32 km^2, and a core area of 0.06 km^2 (Fig. 3). Ninety-five percent of all home-range locations were within habitat classified as dry dipterocarp forest. Non-DDF locations were in edge habitat bordering DDF, except for one location of M1 in dry evergreen forest (Fig. 3).

Micro-habitat selection. We found that both number of small trees and total tree count were negatively associated with mongoose micro-habitat selection (small tree count β = -0.45, SE 0.15, 95% CI -0.77 to -0.17; total tree count β = -0.36, SE 0.13, 95% CI -0.63 to -0.12), based on lowest AICc score (Table 3). Our area under the curve score for our model averaged prediction based on our two top models for micro-habitat selection was 0.52.

The average rodent biomass was highest in core DDF habitat (Core DDF = 215.86 g/ha, SE = 19.47; DDF-dry evergreen edge = 162.27 g/ha, SE = 32.84; DDF-agricultural edge = 160.38 g/ha, SE = 44.49). Arthropod mass was similar in both core DDF (112 g; sweep = 18.1 g) and DDF-agricultural edge (114 g; sweep = 14.7 g), but lowest in the DDF-dry evergreen edge (36.3 g; sweep = 20.9 g). We used a one-way ANOVA to compare rodent density between habitat sections in the DDF, and found that rodent biomass did not significantly differ across the DDF (ANOVA $F_{(2,9)}$ = 0.932, p = 0.43).

We found that small tree count varied significantly within the DDF (Kruskal-Wallis test, chi-squared = 26.51; degrees of freedom = 2, $p < 0.001$). Specifically, a Pairwise Wilcoxon test found that median small tree count was significantly lower in the area of the DDF closest to the dry evergreen edge (2 trees/plot) than the agricultural edge (5 trees/plot) and core DDF zone (5 trees/plot).

Den site selection. We found a total of 36 den site locations from our three mongooses, with two additional sites from a male mongoose (M5) tracked for only two days before his collar fell off. The majority of our den sites were in (available) termite mounds, with only 18% of our dens being dug holes. Den sites had on average 1.7 entrances, a mean width of 11.34 cm, and a mean height of 10.38 cm. Den sites were occupied for an average of 1.6 days, with 30% of sites reused at least once, and one site reused by F1 ten times. The vast majority of our den site reuse was by F1, with a 36% site reuse rate. M1 revisited one den site three

Table 3. Model selection for Javan mongoose (*Herpestes javanicus*) micro-habitat selection at Sakaerat Biosphere Reserve from December 2019 to January 2021, based on logistic regression analysis. Definitions for covariates can be found in Table 1.

Variables	*K*	AICc	ΔAICc	w_i
smallTreeCount	2	435.028	0.000	0.631
totalTrees	2	436.675	1.647	0.277
largeTreeCount	2	441.415	6.387	0.026
shrubCount	2	442.104	6.387	0.018
Constant	1	443.992	8.964	0.007
termiteAvailable	2	444.458	9.430	0.006
FAI	2	445.084	10.056	0.004
avgBasalSmall	2	445.232	10.203	0.004
totalPrey	2	445.583	10.555	0.003
avgBasalSmall + avgBasalLarge +shrubCount	4	445.598	10.570	0.003
termiteNonavailable	2	445.605	10.576	0.003
avgRodentBiomass	2	445.641	10.702	0.003
insectPitfall	2	445.730	10.702	0.003
insectSweep	2	445.852	10.824	0.003
avgBasalLarge	2	445.966	10.938	0.003
holes	2	446.014	10.985	0.003
avgBasalSmall + avgBasalLarge	3	447.264	12.236	0.001
termiteNonavailable + termiteAvailable + holes	4	447.764	12.735	0.001

K is the number of parameters included in the model, AICc is Akaike's Information Criteria corrected for small sample size, ΔAICc is the difference in AICc values, and w_i is the Akaike weight.

times, but otherwise did not reuse sites. M6 only reused a site once. However, site reuse could be underreported, as radio tracking did not typically last more than one hour after sunset when mongoose could still be active. For our den site selection, we found that termite mounds with entry holes were positively associated with mongoose detection (β = 0.69, SE 0.23, 95% CI 0.27–1.17), and that it was the top model for den site selection (Table 4). Our area under the curve score for our top model was 0.71.

We found that total number of termite mounds varied significantly between habitat zones within the DDF (Kruskal-Wallis test, chi-squared = 23.3; degrees of freedom = 2, $p < 0.001$). Specifically a Pairwise Wilcoxon test found that median termite mound count was significantly lower in the area of the DDF closest to the agricultural edge (1 mound/plot) and when compared to core DDF (2 mounds/plot) and DDF adjacent to dry evergreen edge (2 mounds/plot).

DISCUSSION

Our research shows the importance of DDF for Javan mongoose in our study site, as 98% of all of our camera trap detections for Javan mongoose were within DDF. However, as our results are specific to a degraded forest fragment, any comparison to populations inhabiting primary forest should be approached with caution. In addition, while our study clearly shows a preference for more open environments at both the macro- and micro-habitat levels, we are hesitant to say that Javan mongoose are purely open forest specialists based on this study alone, since there are some sparse records of them in evergreen habitat and we only examine one site (Chutipong et al., 2014). Future Javan mongoose studies in other areas of the species range will likely confirm or disprove whether they are specialists.

Our top abundance model showed small tree basal area had the greatest negative effect on mongoose abundance, with distance to edge of the bioreserve having a slightly less, though still quite large, negative effect. Basal area of large trees had the weakest negative effect in our top model. However, these results should be interpreted cautiously as almost all of our detections were from the DDF and all three of the aforementioned covariates were strongly associated with DDF habitat (Petersen et al., 2019). Specifically, DDF in our study site had fewer large trees than dry evergreen, and fewer small trees than either dry evergreen or plantation (Oliver et al., 2019; Petersen et al., 2019). Likewise, the camera traps in the DDF were disproportionately closer to

Table 4. Model selection for Javan mongoose (*Herpestes javanicus*) den site selection at Sakaerat Biosphere Reserve from December 2019 to January 2021, based on logistic regression analysis. Definitions for covariates can be found in Table 1.

Variables	***K***	**AICc**	**ΔAICc**	w_i
termiteAvailable	2	135.547	0.000	0.578
termiteNonavailable + *termiteAvailable* + *holes*	4	136.462	0.914	0.366
constant	1	144.149	8.602	0.008
smallTreeCount	2	144.22	8.673	0.008
termiteNonavailable	2	144.74	9.193	0.006
totalTrees	2	145.194	9.647	0.005
averageBasalLarge	2	145.715	10.168	0.004
averageBasalSmall	2	145.775	10.227	0.003
largeTreeCount	2	145.906	10.359	0.003
insectSweep	2	145.978	10.431	0.003
insectPitfall	2	146.031	10.483	0.003
FAI	2	146.066	10.519	0.003
avgRodentBiomass	2	146.221	10.674	0.003
holes	2	146.222	10.675	0.003
shrubCount	2	146.223	10.676	0.003
avgBasalSmall + *avgBasalLarge*	3	147.518	11.971	0.001
avgBasalSmall + *avgBasalLarge* + *shrubCount*	4	149.656	14.109	0.000

K is the number of parameters included in the model, AICc is Akaike's Information Criteria corrected for small sample size, ΔAICc is the difference in AICc values, and w_i is the Akaike weight.

the edge of the bioreserve compared to those in other habitats as the DDF was restricted to the bioreserve's edge (Fig. 1).

Because this is the first study on Javan mongoose abundance and spatial ecology, we use the closest living relative to the Javan mongoose (Veron et al., 2007), the grey mongoose (*Herpestes edwardsii*) as a metric for comparison. Grey and Javan mongoose both appear to have similar selection for open dry forests, so their ecology may be comparable (Kalle et al., 2013, 2014; Bajaru et al., 2020). Grey mongoose mean abundance, estimated using the RN model in a non-fragmented forest over two years, was lower (λ_{mean} = 0.34 [95% CI 0.026–0.654] to 0.68 [95% CI 0.006–1.366]; Kalle et al., 2014) but otherwise similar to our overall estimates for Javan mongoose in a forest fragment (λ_{mean} = 1.10, 95% CI 0.65–1.92). However, grey mongoose estimates were closer to Javan mongoose estimates in closed forests (λ_{mean} = 0.36, 95% CI 0.18–0.78) than those in the DDF (λ_{mean} = 3.04, 95% CI 1.97–4.96). This is possibly due to grey mongoose abundance being clustered in smaller patches of open dry habitat, similar to our species. This would cause lambda averaged across large forest matrixes to appear misleadingly low. In addition, grey mongoose abundance could be higher within fragmented forests, as is the case for some mongoose species (Mudappa et al., 2007).

Our home-range estimations suggest a difference between male and female area utilisation, with the female using only 14.5% of the average male's home-range size, although our low sample size means we cannot ascertain the representativeness of our observations compared to either the population or the species as a whole (Fig. 3). Nevertheless, this observation appears to support our prediction that males would use a larger area than females, presumably to increase reproductive access by having their range overlap with several females (Emlen & Oring, 1977; Greenwood, 1980). The sex-based difference in home-range size may also contribute to our male trapping bias, as a larger home-range allows for overlap with several trapping stations, while a female's smaller range may not encompass traps unless they are relatively near the individual's activity centre. Sexual dimorphism in home-range size of small mustelid species results in similar trapping bias towards males (Buskirk & Lindstedt, 1989). Similarly, the short-tailed mongoose (*Herpestes brachyurus*) also shows larger home-ranges in males (mean = 2.33 km^2) than females (mean = 1.32 km^2) (Jennings et al., 2010). Home-range data on other Asian mongoose species is lacking, with the only available data for grey mongoose based on one individual and 21 locations (0.155 km^2), and therefore probably underestimated (Kumar & Umapathy, 1999).

In congruence with our abundance results, our micro-habitat selection data shows that individual mongooses were associated with areas with low numbers of small trees (Table 3). This indicates a selection within DDF for more open areas with less small woody regrowth. It may also imply a preference for mature forests, which tend to have larger widely spaced trees (Hamer et al., 2003; Watson et al., 2004). We found significantly less small trees and more termite mounds in DDF habitat closer to the interior of the reserve (DDF-dry evergreen edge) than in DDF along its agricultural edge. This could be due to fire suppression by reserve staff, who patrol the edges of the DDF during yearly burns and discourage high fire intensity near the edge of the reserve to prevent spread to agricultural areas. Reduced burning in DDF can increase tree density and decrease *macrotermitinae* species richness (Davies, 1997; Wood, 2012). Another cause might be historical harvesting for charcoal production near the edge of the reserve, since charcoal harvesters often remove larger trees (Aabeyir et al., 2016) which would create space for a greater density of small trees once the reserve was protected. Likely several additive factors contribute to the difference in microhabitat structure. Javan mongoose did not select for microhabitats with higher den site counts as we predicted, but termite mounds were overwhelmingly selected as den sites by mongoose over dug holes, and hollow termite mounds were our top model for den site specific selection (Table 4). Rather than select for termite mounds on the micro-habitat scale, our tracked mongoose may have selected on a home-range level for sections of the DDF where den sites were more available. However, we cannot be certain if that is the case.

Neither overall prey biomass nor rodent specific biomass appeared to influence mongoose micro-habitat selection, so our prediction that mongoose would select for areas with higher prey biomass was not supported (Table 3). However, we did not find a significant difference in rodent biomass between different DDF habitat zones, suggesting the availability of rodents may have been relatively uniform across the small DDF patch we investigated. Moreover, mongoose are generalist predators (Subrata et al., 2021), and therefore have the ability to shift their diets in response to resource availability, so they may simply have prioritised other more abundant prey when rodents or arthropod abundance were low, rather than adjust their range to match. Finally, the low predictive ability of our micro-habitat selection model (AUC 0.52) is likely a reflection of the relatively homogenous landscape of the DDF selected for by mongoose.

The status of Javan mongoose populations in other natural open habitat or in agriculture is not known. Understanding the level of dependence Javan mongoose have on open habitat is urgent for conservation, as open habitats are underrepresented in Thailand's current protected area system (Tantipisanuh & Gale, 2013) and are often mislabelled as degraded forests of low conservation priority (Ratnam et al., 2016). Open forests also face unique threats such as invasion by woody species (Stevens et al., 2017) compounded by inappropriate fire management strategies (O'Connor et al., 2014; Moura et al., 2019) and a lack of traditional large herbivores (Daskin et al., 2016). If Javan mongoose are as selective to open habitat as our study suggests, similar open habitats across Southeast Asia, such as pine savannahs or mixed teak forest, may serve as reservoirs for the species. Camera trap surveys specific to open forest habitat will likely provide valuable insight on the status of current Javan mongoose populations.

ACKNOWLEDGEMENTS

Thank you to Sakaerat Biosphere Reserve's director Surachit Waengsothorn. We would also like to thank Jirayut Iemnok, Kanoktip Somsiri, Phonnapa Luekhamhan, Marisa Pringproh, Shannon Thrasher, Samantha Jones, and Dayna Levine for their assistance in the field. Thanks to Diane Turner, Jack Sherburne, and Mimi Sherburne for their support. Funding was provided by Thailand's National Science and Technology Development Agency (grant number P-17-50347) and the Association of Tropical Biology Conservation.

LITERATURE CITED

Aabeyir R, Adu-Bredu S, Agyare WA & Weir MJ (2016) Empirical evidence of the impact of commercial charcoal production on Woodland in the Forest-Savannah transition zone, Ghana. Energy for Sustainable Development 33: 84–95.

Bajaru S, Pal S, Mrugank P, Patel P, Khot R & Apte D (2020) A multi-species occupancy modeling approach to access the impacts of land use and land cover on terrestrial vertebrates in the Mumbai Metropolitan Region (MMR), Western Ghats, India. PLoS ONE, 15(10): e0240989.

Bates D, Mächler M, Bolker B & Walker S (2015) Fitting linear mixed-effects models using lme4. Journal of Statistical Software, 67(1): 1–48.

Borchers DA (2012) A non-technical overview of spatially explicit capture–recapture models. Journal of Ornithology, 152(2): 435–444.

Brooke ZM, Bielby J, Nambiar K & Carbone C (2014) Correlates of research effort in carnivores: body size, range size and diet matter. PLoS ONE, 9(4): e93195.

Burnham KP & Anderson DR (1998) Practical Use of the Information-Theoretic Approach. In: Model Selection and Inference. Springer, New York, pp. 75–117.

Burnham KP, Anderson DR & Huyvaert KP (2011) AIC model selection and multimodel inference in behavioral ecology: some background, observations, and comparisons. Behavioral Ecology and Sociobiology, 65: 23–35.

Buskirk SW & Lindstedt SL (1989) Sex biases in trapped samples of Mustelidae. Journal of Mammalogy, 70(1): 88–97.

Calabrese JM, Fleming CH & Gurarie E (2016) ctmm: an R package for analyzing animal relocation data as a continuous time stochastic process. Methods in Ecology and Evolution, 7(9): 1124–1132.

Case TJ & Bolger DT (1991) The role of interspecific competition in the biogeography of island lizards. Trends in Ecology & Evolution, 6(4): 135–139.

Chutipong W, Tantipisanuh N, Ngoprasert D, Lynam AJ, Steinmetz R, Jenks KE, Grassman LI, Tewes M, Kitamura S, Baker MC, McShea W, Bhumpakphan N, Sukmasuang R, Gale GA, Harish FK, Treydte AC, Cutter P, Cutter PB, Suwanrat S, Siripattaranukul K, Hala-Bala Wildlife Research Station, Wildlife Research Division & Duckworth JW (2014) Current

distribution and conservation status of small carnivores in Thailand: a baseline review. Small Carnivore Conservation, 51: 96–136.

Chutipong W, Duckworth JW, Timmins R, Willcox DHA & Ario A (2016) *Herpestes javanicus*. The IUCN Red List of Threatened Species, 2016: e.T70203940A45207619. https://dx.doi.org/10.2305/IUCN.UK.2016-1.RLTS.T70203940A45207619.en (Accessed 3 November 2021).

Daskin JH, Stalmans M & Pringle RM (2016) Ecological legacies of civil war: 35 year increase in savanna tree cover following wholesale large mammal declines. Journal of Ecology, 104(1): 79–89.

Davies RG (1997) Termite species richness in fire-prone and fire-protected dry deciduous dipterocarp forest in Doi Suthep-Pui National Park, northern Thailand. Journal of Tropical Ecology, 13(1): 153–160.

Delciellos AC, Suzy ER & Vieira MV (2017) Habitat fragmentation effects on fine-scale movements and space use of an opossum in the Atlantic Forest. Journal of Mammalogy, 98(4): 1129–1136.

Deuel NR, Conner LM, Miller KV, Chamberlain MJ, Cherry MJ & Tannenbaum LV (2017) Habitat selection and diurnal refugia of gray foxes in southwestern Georgia, USA. PLoS ONE, 12(10): 1–12.

Duckworth JW, Timmins RJ & Tizard T (2010) Conservation status of Small Asian Mongoose *Herpestes javanicus* (E. Geoffroy Saint-Hilaire, 1818) (Mammalia: Carnivora: Herpestidae) in Lao PDR. Raffles Bulletin of Zoology, 58(2): 403–410.

Efford MG (2021) Secr: Spatially Explicit Capture-recapture Models. R Package Version 4.4.5. http://CRAN.R-project.org/package=secr (Accessed 1 November 2021).

Emlen ST & Oring LW (1977) Ecology, sexual selection, and the evolution of mating systems. Science, 197(4300): 215–223.

Estoque RC, Ooba M, Avitabile V, Hijioka Y, DasGupta R, Togawa T & Murayama Y (2019) The future of Southeast Asia's forests. Natural Communication, 10(1): 1–12.

Ferreras P, Francisco DT & Monterroso P (2018) Improving mesocarnivore detectability with lures in camera-trapping studies. Wildlife Research, 45(6): 505–517.

Filla M, Premier J, Magg N, Dupke C, Khorozyan I, Waltert M, Bufka L & Heurich M (2017) Habitat selection by Eurasian lynx (*Lynx lynx*) is primarily driven by avoidance of human activity during day and prey availability during night. Ecology and Evolution, 7(16): 6367–6381.

Fiske I & Chandler R (2011) unmarked: An R package for fitting hierarchical models of wildlife occurrence and abundance. Journal of Statistical Software, 43(10): 1–23.

Fleming CH, Calabrese JM, Mueller T, Olson KA, Leimgruber P & Fagan WF (2014) From fine-scale foraging to home ranges: a semivariance approach to identifying movement modes across spatiotemporal scales. The American Naturalist, 183(5): E154–E167.

Fleming CH, Fagan WF, Mueller T, Olson KA, Leimgruber P & Calabrese JM (2015) Rigorous home range estimation with movement data: a new autocorrelated kernel density estimator. Ecology, 96(5): 1182–1188.

Freeman EA & Moisen G (2008) PresenceAbsence: An R package for presence-absence model analysis. Journal of Statistical Software, 23(11): 1–31.

Gerber BD, Karpanty SM & Kelly MJ (2012) Evaluating the potential biases in carnivore capture–recapture studies associated with the use of lure and varying density estimation techniques using photographic-sampling data of the Malagasy civet. Population Ecology, 54(1): 43–54.

Grantham HS, Duncan A, Evans TD, Jones KR, Beyer HL, Schuster R, Walston J, Ray JC, Robinson JG, Callow M, Clements T, Costa HM, DeGemmis A, Elsen PR, Ervin J, Franco P, Goldman E, Goetz S, Hansen A, Hofsvang E, Jantz P, Jupiter S, Kang A, Langhammer P, Laurance WF, Lieberman S, Linkie M, Malhi Y, Maxwell S, Mendez M, Mittermeier R, Murray NJ, Possingham H, Radachowsky J, Saatchi S, Samper C, Silverman J, Shapiro A, Strassburg B, Stevens T, Stokes E, Taylor R, Tear T, Tizard R, Venter O, Visconti P, Want S & Watson JEM (2020) Anthropogenic modification of forests means only 40% of remaining forests have high ecosystem integrity. Nature Communications, 11(1): 5978.

Greenwood PJ (1980) Mating systems, philopatry and dispersal in birds and mammals. Animal Behaviour, 28(4): 1140–1162.

Hamer KC, Hill JK, Benedick S, Mustaffa N, Sherratt TN & Maryati MT (2003) Ecology of butterflies in natural and selectively logged forests of northern Borneo: the importance of habitat heterogeneity. Journal of Applied Ecology, 40(1): 150–162.

Hinton JW, Proctor C, Kelly MJ, Van Manen FT, Vaughan MR & Chamberlain MJ (2016) Space use and habitat selection by resident and transient red wolves (*Canis rufus*). PLoS ONE, 11(12): e0167603.

Holinda D, Burgar JM & Burton AC (2020) Effects of scent lure on camera trap detections vary across mammalian predator and prey species. PLoS ONE, 15(5): e0229055.

Jennings AP, Zubaid A & Veron G (2010) Home ranges, movements and activity of the short-tailed mongoose (*Herpestes brachyurus*) on Peninsular Malaysia. Mammalia, 74: 43–50.

Kalle R, Ramesh T, Qureshi Q & Sankar K (2013) Predicting the distribution pattern of small carnivores in response to environmental factors in the Western Ghats. PLoS ONE, 8(11): e79295.

Kalle R, Ramesh T, Qureshi Q & Sankar K (2014) Estimating seasonal abundance and habitat use of small carnivores in the Western Ghats using an occupancy approach. Journal of Tropical Ecology, 30(5): 469–480.

Khamcha D, Corlett RT, Powell LA, Savini T, Lynam AJ & Gale GA (2018) Road induced edge effects on a forest bird community in tropical Asia. Avian Research, 9(1): 1–13.

Kumar A & Umapathy G (1999) Home range and habitat use by Indian grey mongoose and small Indian civets in Nilgiri Biosphere Reserve, India. In: Hussain SA (ed.) ENVIS Bulletin: Wildlife and Protected Areas, Mustelids, Viverrids and Herpestids of India, Wildlife Institute of India: 87–91.

Lowe S, Browne M, Boudjelas S & Poorter MD (2004) 100 of the world's worst invasive alien species. A selection from the global invasive species database. Invasive Species Specialist Group, Auckland, New Zealand, 11 pp.

Mace GM, Collar NJ, Gaston KJ, Hilton Taylor C, Akçakaya HR, Leader Williams N, Milner Gulland EJ & Stuart SN (2008) Quantification of extinction risk: IUCN's system for classifying threatened species. Conservation Biology, 22(6): 1424–1442.

MacKenzie DI & Bailey LL (2004) Assessing the fit of site-occupancy models. Journal of Agricultural, Biological, and Environmental Statistics, 9(3): 300–318.

Marneweck C, Butler AR, Gigliotti LC, Harris SN, Jensen AJ, Muthersbaugh M, Newman A, Saldo EA, Shute K, Titus KL, Yu SW & Jachowski DS (2021) Shining the spotlight on small mammalian carnivores: global status and threats. Biological Conservation, 255: 109005.

Mazerolle MJ (2020) AICcmodavg: Model selection and multimodel inference based on (Q)AICI. R Package Version 2.3-1. https://cran.r-project.org/package=AICcmodavg (Accessed 8 November 2021).

McPherson FJ & Chenoweth PJ (2012) Mammalian sexual dimorphism. Animal Reproduction Science, 131(3–4): 109–122.

Moehrenschlager A, List R & Macdonald DW (2007) Escaping intraguild predation: Mexican kit foxes survive while coyotes and golden eagles kill Canadian swift foxes. Journal of Mammalogy, 88(4): 1029–1039.

Moura LC, Scariot AO, Schmidt IB, Beatty R & Russell-Smith J (2019) The legacy of colonial fire management policies on traditional livelihoods and ecological sustainability in savannas: impacts, consequences, new directions. Journal of Environmental Management, 232: 600–606.

Mudappa D, Noon BR, Kumar A & Chellam R (2007) Responses of small carnivores to rainforest fragmentation in the southern Western Ghats, India. Small Carnivore Conservation, 36: 18–26.

Nakashima Y (2020) Potentiality and limitations of *N* mixture and Royle Nichols models to estimate animal abundance based on noninstantaneous point surveys. Population Ecology, 62(1): 151–157.

Noonan MJ, Tucker MA, Fleming CH, Akre TS, Alberts SC, Ali AH, Altmann J, Antune PC, Belant JL, Beyer D, Blaum N, Bohning-Gaese K, Cullen Jr L, de Paula RC, Dekker J, Drescher-Lehman JD, Farwig N, Fichtel C, Fischer C, Ford A, Goheen JR, Janssen R, Jeltsch F, Kauffman M, Kappeler PM, Koch F, LaPoint S, Markham AC, Medici EP, Morato RG, Nathan R, Oliveira-Santos LGR, Olson KA, Pattersoh BD, Paviolo A, Ramalho EE, Roesner S, Schabo D, Selva N, Sergiel A, da Silva X, Spiegel O, Thompson P, Ullmann W, Zieba F, Zwijacz-Kozica T, Fagan WF, Mueller T & Calabrese JM (2019) A comprehensive analysis of autocorrelation and bias in home range estimation. Ecological Monographs, 89(2): e01344.

O'Brien TG, Kinnaird MF & Wibisono HT (2003) Crouching tigers, hidden prey: Sumatran tiger and prey populations in a tropical forest landscape. Animal Conservation, 6: 131–139.

O'Connor CD, Falk DA, Lynch AM & Swetnam TW (2014) Fire severity, size, and climate associations diverge from historical precedent along an ecological gradient in the Pinaleño Mountains, Arizona, USA. Forest Ecology and Management, 329: 264–278.

Oliver K, Ngoprasert D & Savini T (2019). Slow loris density in a fragmented, disturbed dry forest, nort east Thailand. American Journal of Primatology, 81(3): e22957.

Ongsomwang S & Sutthivanich I (2014) Integration of remotely sensed data and forest landscape pattern analysis in Sakaerat Biosphere Reserve. Suranaree Journal of Science and Technology, 21(3): 233–248.

Owen MA & Lahti DC (2020) Rapid evolution by sexual selection in a wild, invasive mammal. Evolution, 74(4): 740–748.

Paolino RM, Royle JA, Versiani NF, Rodrigues TF, Pasqualotto N, Krepschi VG & Chiarello AG (2018) Importance of riparian forest corridors for the ocelot in agricultural landscapes. Journal of Mammalogy, 99(4): 874–884.

Paradis E & Schliep K (2019) ape 5.0: an environment for modern phylogenetics and evolutionary analyses in R. Bioinformatics, 35: 526–528.

Petersen WJ, Savini T, Steinmetz R & Ngoprasert D (2019) Periodic resource scarcity and potential for interspecific competition influences distribution of small carnivores in a seasonally dry tropical forest fragment. Mammalian Biology, 95(1): 112–122.

R Core Team (2020) R: A language and environment for statistical computing. R Foundation for Statistical Computing, Vienna, Austria. https://www.R-project.org/ (Accessed 8 November 2021).

Ramesh T, Kalle R & Downs CT (2017) Space use in a South African agriculture landscape by the caracal (*Caracal caracal*). European Journal of Wildlife Research, 63(1): 1–11.

Ratnam J, Tomlinson KW, Rasquinha DN & Sankaran M (2016) Savannahs of Asia: antiquity, biogeography, and an uncertain future. Philosophical Transactions of the Royal Society B: Biological Sciences, 371(1703): 20150305.

Royle JA & Nichols JD (2003) Estimating abundance from repeated presence–absence data or point counts. Ecology, 84(3): 777–790.

Sikes RS & Gannon WL (2011) Guidelines of the American Society of Mammalogists for the use of wild mammals in research. Journal of Mammalogy, 92(1): 235–253.

Simberloff D, Dayan T, Jones C & Ogura G (2000) Character displacement and release in the small Indian mongoose, *Herpestes javanicus*. Ecology, 81(8): 2086–2099.

Sodhi NS, Posa MRC, Lee TM, Bickford D, Koh LP & Brook BW (2010) The state and conservation of Southeast Asian biodiversity. Biodiversity and Conservation, 19(2): 317–328.

Stevens N, Lehmann CER, Murphy BP & Durigan G (2017) Savanna woody encroachment is widespread across three continents. Global Change Biology, 23(1): 235–244.

Subrata SA, Siregar SRT, André A & Michaux JR (2021) Identifying prey of the Javan mongoose (*Urva javanica*) in Java from fecal samples using next-generation sequencing. Mammalian Biology, 101(1): 63–70.

Suraci JP, Clinchy M, Dill LM, Roberts D & Zanette LY (2016) Fear of large carnivores causes a trophic cascade. Nature Communications, 7(1): 1–7.

Tannerfeldt M, Moehrenschlager A & Angerbjörn A (2003) Den Ecology of Swift, Kit and Arctic Foxes: A Review. In: Sovada M & Carbyn L (eds.) Ecology and Conservation of Swift Foxes in a Changing World. Canadian Plains Research Center, University of Regina, pp. 167–181.

Tantipisanuh N & Gale GA (2013) Representation of threatened vertebrates by a protected area system in southeast Asia: the importance of non-forest habitats. Raffles Bulletin of Zoology, 61(1): 359–395.

Taubert F, Fischer R, Groeneveld J, Lehmann S, Müller MS, Rödig E, Wiegand T & Huth A (2018) Global patterns of tropical forest fragmentation. Nature, 554(7693): 519–522.

Vanbianchi CM, Melanie AM & Karen EH (2017) Canada lynx use of burned areas: conservation implications of changing fire regimes. Ecology and Evolution, 7(7): 2382–2394.

Veron G & Jennings AP (2017) Javan mongoose or small Indian mongoose–who is where? Mammalian Biology, 87(1): 62–70.

Veron G, Patou ML, Pothet G, Simberloff D & Jennings AP (2007) Systematic status and biogeography of the Javan and small Indian mongooses (Herpestidae, Carnivora). Zoologica Scripta, 36(1): 1–10.

Watson JEM, Whittaker RJ & Dawson TP (2004) Habitat structure and proximity to forest edge affect the abundance and distribution of forest-dependent birds in tropical coastal forests of southeastern Madagascar. Biological Conservation, 120(3): 311–327.

Wei T & Simko V (2021) R package "corrplot": Visualization of a Correlation Matrix. (Version 0.88). https://github.com/taiyun/corrplot (Accessed 8 November 2021).

Wilcove DS, Giam X, Edwards DP, Fisher B & Koh LP (2013) Navjot's nightmare revisited: logging, agriculture, and biodiversity in Southeast Asia. Trends in Ecology and Evolution, 28: 531–540.

Wolff PJ, Taylor CA, Heske EJ & Schooley RL (2015) Habitat selection by American mink during summer is related to hotspots of crayfish prey. Wildlife Biology, 21(1): 9–17.

Wood TF (2012) Fire ecology of the dry dipterocarp forests of South West Cambodia. Cambodian Journal of Natural History, 2012(1): 64–74.

Zoletil the Versatile Anaesthetic (2011) Virbac Animal Health India PVT LTD. https://in.virbac.com/files/live/sites/virbac-in/files/predefined-files/PDF%20documents/Zoletil%20-%20Wildlfe%20dosage%20guidelines.pdf (Accessed 23 August 2021).

APPENDIX

Appendix 1. Morphological data for Javan mongoose (*Herpestes javanicus*) trapped within Sakaerat Biosphere Reserve.

ID	Sex	Age class	Tail length (cm)	Body length (cm)	Mass (g)	Circumference of neck (cm)	Circumference of skull at mandible (cm)	Hind paw width (cm)	Front paw width (cm)
M1	male	adult	35.5	45.0	1055	14.1	15.1	2.3	2.2
M2	male	adult	33.0	30.0	1130	14.2	14.9	1.3	1.2
M3	male	young adult	34.6	30.5	720	12.5	13.2	1.9	1.9
F1	female	young adult	38.0	32.0	600	10.2	11.4	1.2	1.2
M4	male	adult	35.2	33.5	710	11.7	14.4	2.0	2.4
M5	male	adult	33.1	36.4	1250	15.5	16.8	2.5	2.5
M6	male	adult	31.5	41.2	1100	14.5	15.9	2.4	2.2

Appendix 2. Immobilisation dosing and details of Javan mongoose (*Herpestes javanicus*) trapped within Sakaerat Biosphere Reserve.

We anaesthetised Javan mongoose (*Herpestes javanicus*) using Zoletil™ 100 for injection (tiletamine and zolazepam). The addition of 5 ml diluent produces a solution containing the equivalent of 50 mg tiletamine base, 50 mg zolazepam base, and 57.7 mg mannitol per millilitre. This solution has a pH of 2 to 3.5 and is recommended for deep intramuscular injection. The doses used in this study were 5.0 mg/kg intramuscular injections (personal recommendation by Doctor Marnoch Yindee).

Average anaesthesia duration of each individual lasted 60–180 minutes longer than recommended by Virbac pharmaceutical company (20–60 min). We recommend for future researchers to reduce the dose to 4.4 mg/kg as recommended for black-footed mongoose (*Bdeogale nigripes*) (Zoletil the Versatile Anaesthetic, 2021). We prepared Doxapram and Yohimbine HCI as an antidote of tilemine and zolazepam in case of accidental overdose.

Appendix 3. Spatially explicit capture-recapture models for small and large mass species group rodent densities. Behavioural effects tested: ~b, change in behaviour after first capture; ~B, change in behaviour depending on capture previous occasion; ~bk, trap-specific lingering response post initial capture; ~Bk, trap-specific response post capture.

Small Mass Species (< 50 g)				
variables	***K***	**AICc**	**ΔAICc**	w_i
D~session, g0~bk, sigma~1	13	2515.00	0.00	1.00
D~session, g0~b, sigma~1	13	2527.07	12.07	0.00
D~session, g0~Bk, sigma~1	13	2541.35	26.35	0.00
D~session, g0~B, sigma~1	13	2543.31	28.31	0.00
D~session, g0~1, sigma~1	12	2563.13	48.13	0.00
D~session, g0~session, sigma~session	30	2576.59	61.59	0.00
D~1, g0~1, sigma~1	3	2610.19	95.19	0.00
Large Mass Species (> 50 g)				
D~session, g0~Bk, sigma~1	13	2823.71	0.00	0.94
D~session, g0~b, sigma~1	13	2830.63	6.92	0.03
D~session, g0~bk, sigma~1	13	2830.68	6.97	0.03
D~session, g0~B, sigma~1	13	2847.27	23.56	0.00
D~session, g0~1, sigma~1	12	2849.13	25.42	0.00
D~1, g0~1, sigma~1	3	2869.55	45.84	0.00
D~session g0~session sigma~session	30	2870.70	46.99	0.00

K is the number of parameters included in the model, AICc is Akaike's Information Criteria corrected for small sample size, ΔAICc is the difference in AICc values, and w_i is the Akaike weight.